Interfacial Charge-Transfer in CoAl–LDH/CoO_x for Photocatalytic Dye Degradation and UV/H_2O_2 assisted Real-Wastewater Treatment

Tariq Ali,[a,b] Yiwei Li,[a,b] Bingjie Fang,[a,b] Saleem Raza, [*c] Yeyuan Xiao[a,b *]

[a]Department of Civil Engineering and Smart Cities, Shantou University, Shantou, Guangdong 515063, China.

[b]Guangdong Engineering Technology Research Center of Offshore Environmental Pollution Control, Shantou University, Shantou, Guangdong 515063, China.

[c]College of Geography and Environmental Sciences, Zhejiang Normal University, Jinhua 321004, PR China.

[*]Corresponding authors

Emails: raza88@zjnu.edu.cn (SR) yeyuanxiao@stu.edu.cn (YX)

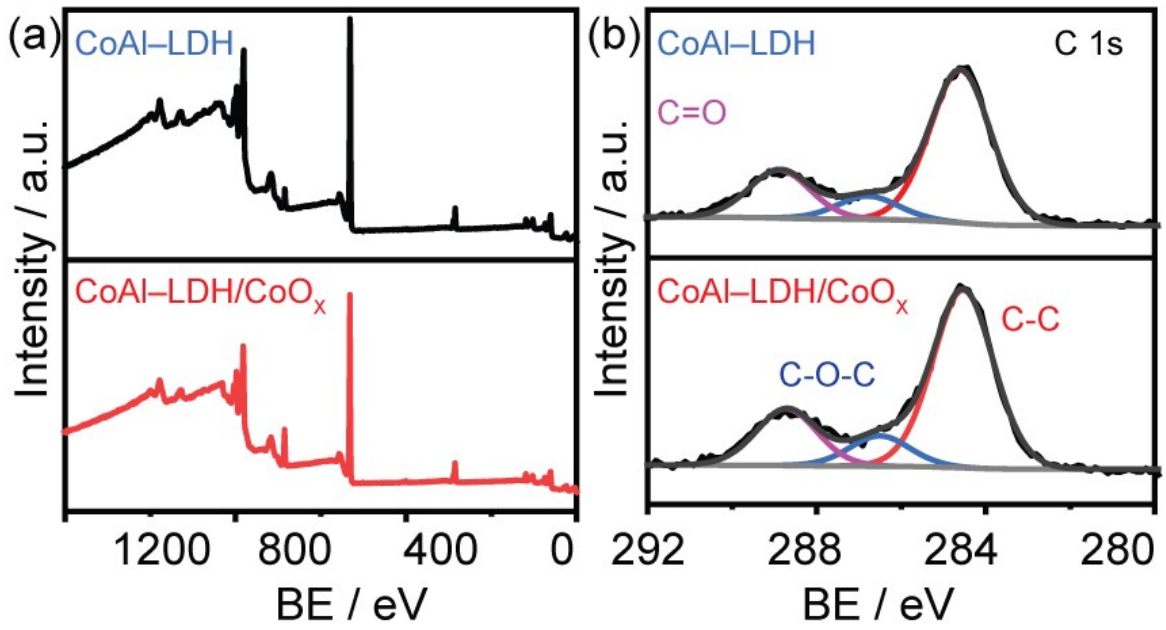

Fig. S1. Characterizations of the pristine CoAl–LDH and CoAl–LDH/CoOx (a) XPS survey spectra (b) C 1s spectra.

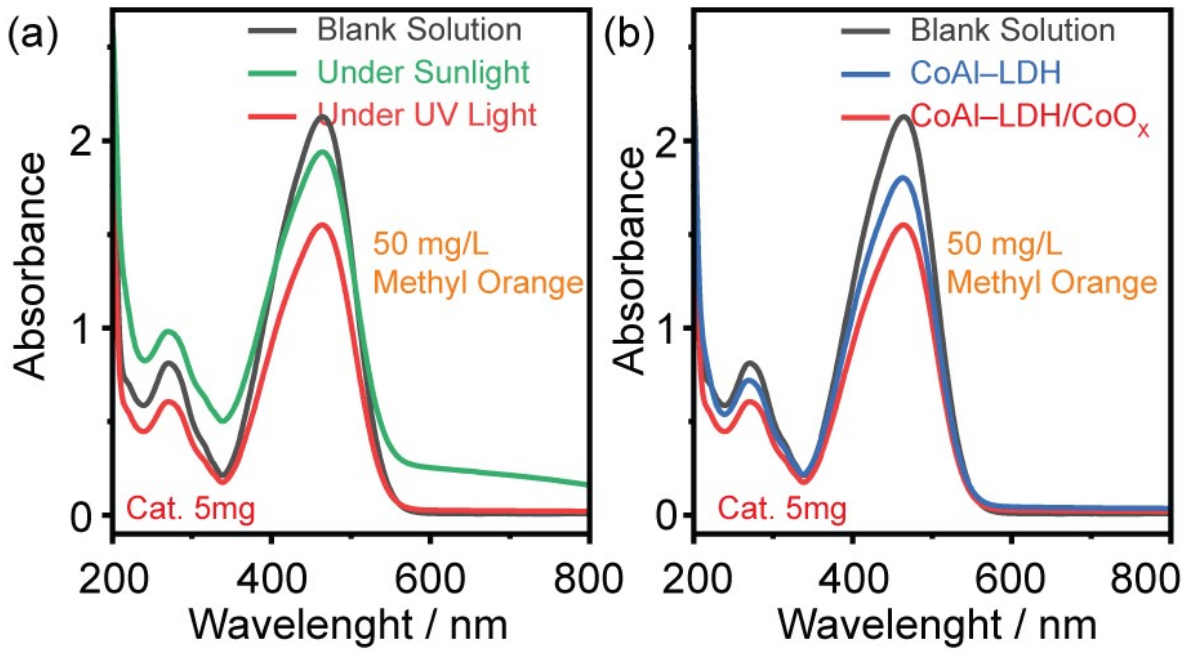

Fig. S2. Photocatalytic Performance of CoAl–LDH/CoO_x and CoAl–LDH. (a) UV-vis spectra of methyl orange in the presence of CoAl–LDH/CoO_x photocatalyst with an initial concentration of 50 mg/L during degradation with UV light and sunlight. (b) UV-vis spectra of methyl orange in the presence of CoAl–LDH/CoO_x and CoAl–LDH with an initial concentration of 50 mg/L during degradation.

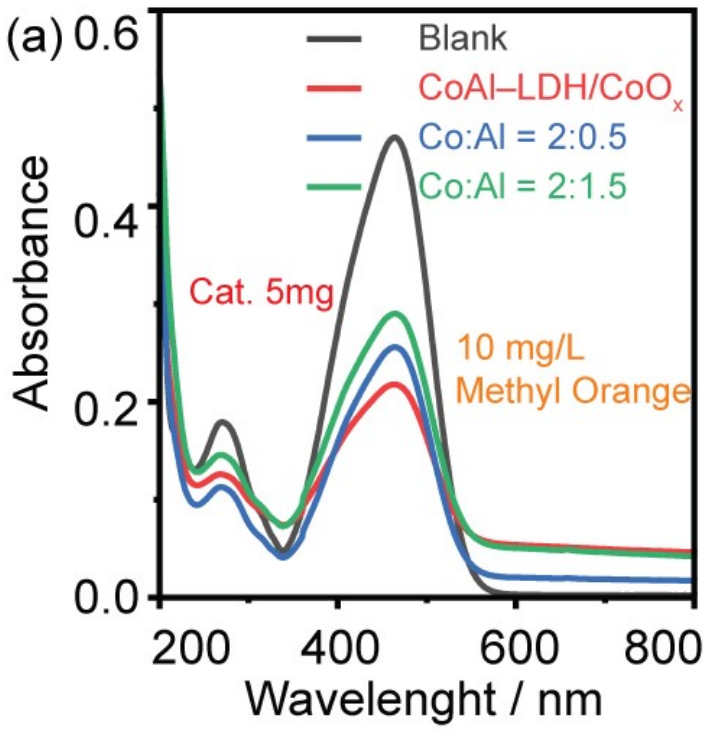

Fig. S3. Photocatalytic Performance of CoAl–LDH/CoOx, Co:Al = 2:0.5 and Co:Al = 2:1.5.

UV-vis spectra of methyl orange with an initial concentration of 10 mg/L during degradation.

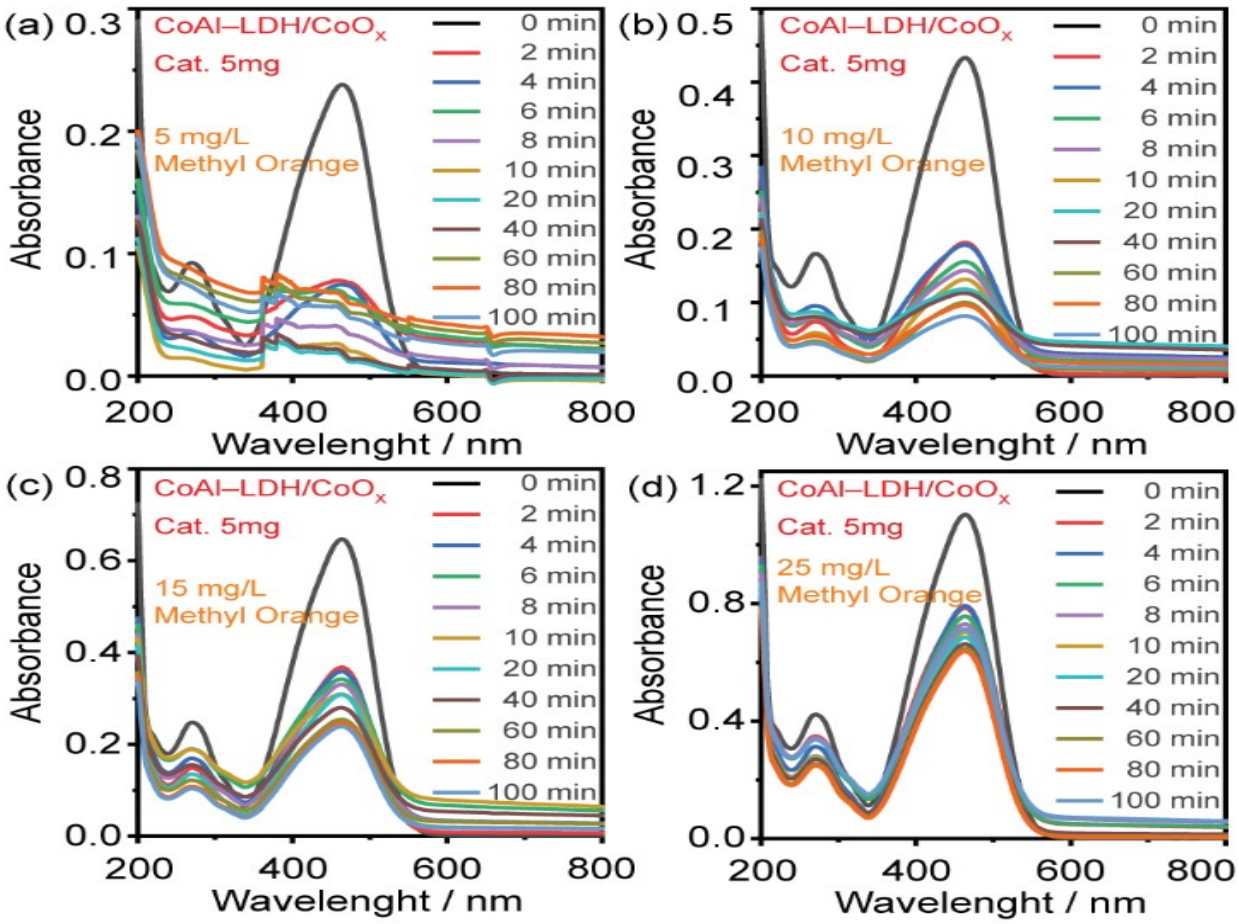

Fig. S4. Photocatalytic Performance of CoAl–LDH/CoOx. UV-vis spectra of methyl orange for a time duration of 100 min with an initial concentration of (a) 5 mg/L during degradation, (b) 10 mg/L during degradation. (c) 15 mg/L during degradation, (d) 25 mg/L during degradation.

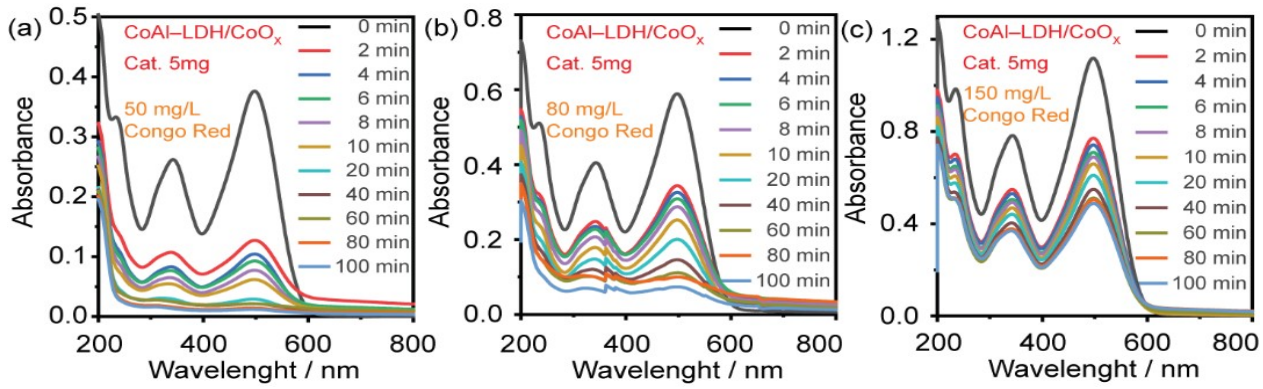

Fig. S5. Photocatalytic Performance of CoAl–LDH/CoOx. UV-vis spectra of Congo red for a time duration of 100 min with an initial concentration of (a) 50 mg/L during degradation, (b) 80 mg/L during degradation. (c) 150 mg/L during degradation.

In this work, the band positions used in the schematic alignment diagram (Fig. 12) were obtained by combining our experimental band-gap data with reported band-edge information from the literature. Specifically, the optical band gaps (E_g) of CoAl–LDH and CoO_x were estimated from UV–Vis diffuse reflectance spectra using Tauc plots based on the Kubelka–Munk function (Fig. 4b). Using these E_g values together with previously reported conduction- and valence-band edge positions (or electronegativity-based estimates) for CoAl–LDH and cobalt oxides, we constructed a qualitative band alignment that is consistent with the observed PL quenching and the h^+/$\bullet O_2^-$-dominated mechanism inferred from scavenger and EPR experiments. The diagram in Fig. 12 is therefore intended as a schematic illustration of the relative band positions and interfacial charge-transfer pathway, rather than an exact measurement of absolute band-edge energies.

The band positions in Fig. 12 were estimated theoretically by combining the experimentally determined band gap with the Mulliken electronegativity approach, which is widely used for semiconductor photocatalysts.[1–3]

First, the optical band gap (Eg) of the CoAl–LDH/CoO_x composite was obtained from UV–vis diffuse reflectance spectra using the Kubelka–Munk function and Tauc analysis. Plotting $F(R)\cdot h\nu^{1/2}$ versus

$h\nu$ and extrapolating the linear region to $F(R)\cdot h\nu^{1/2} = 0$ gave $E_g \approx 3.77$ eV for CoAl–LDH/CoO_x (Fig. 4b).

The valence-band (E_{VB}) and conduction-band (E_{CB}) edge potentials *vs.* the normal hydrogen electrode (NHE) were then estimated using the Mulliken electronegativity equations: [1–3]

$$E_{VB} = X - Ee + \tfrac{1}{2} Eg$$

$$E_{CB} = E_{VB} - E_g$$

where X is the absolute electronegativity of the semiconductor, Ee is the energy of free electrons on the hydrogen scale (Ee ≈ 4.5 eV), and Eg is the optical band gap. For CoAl-LDH-based materials, an absolute electronegativity of X ≈ 5.85 eV has been reported in recent g-C_3N_4/CoAl-LDH heterostructure studies.[4] Assuming that the CoAl–LDH/CoO_x composite inherits the CoAl-LDH–dominated band centre with only modest shifts from CoO_x nanoclusters, we used X = 5.85 eV for the band-edge estimate. Substituting the experimental E_g and X gives:

$$E_{VB} = 5.85 - 4.50 + \tfrac{1}{2} \times 3.77 = 1.35 + 1.885 \approx 3.24 \text{ V vs. NHE}$$

$$E_{CB} = 3.24 - 3.77 \approx -0.53 \text{ V vs. NHE}$$

Thus, the CoAl–LDH/CoO_x composite is estimated to have $E_{CB} \approx -0.53$ V and $E_{VB} \approx +3.24$ V *vs.* NHE. The conduction band is more negative than the $O_2/\bullet O_2^-$ redox couple ($E°(O_2/\bullet O_2^-) \approx -0.33$ V vs. NHE), while the valence band is more positive than the OH/•OH and H_2O/•OH redox potentials (≈ +1.99 –2.7 V vs. NHE).[5,6] These positions support the mechanism proposed in Fig. 12: photogenerated electrons in the CB can reduce dissolved O_2 to $\bullet O_2^-$, and photogenerated holes in the VB can directly oxidize dyes and/or surface –OH groups (with •OH becoming more important in the presence of H_2O_2).

1. Di Paola, Agatino, et al. "A survey of photocatalytic materials for environmental remediation." Journal of hazardous materials 211 (2012): 3-29.

2. Rasheed-Adeleke, Azeezat A., et al. "Enhanced photocatalytic degradation of tetracycline using $Ag_3PO_4/ZnFe_2O_4$ composite." Applied Physics A 131.11 (2025): 1-11.

3. Chen, Xiaobo, et al. "Semiconductor-based photocatalytic hydrogen generation." Chemical reviews 110.11 (2010): 6503-6570.

4. Jo, Wan-Kuen, and Surendar Tonda. "Novel CoAl-LDH/g-C_3N_4/rGO ternary heterojunction with notable 2D/2D/2D configuration for highly efficient visible-light-induced photocatalytic elimination of dye and antibiotic pollutants." Journal of hazardous materials 368 (2019): 778-787.

5. Wang, Kai, et al. "Hexagonal CdS single crystals coupled with layered CoAl LDH—a step-scheme heterojunction for efficient photocatalytic hydrogen evolution." Journal of Sol-Gel Science and Technology 107.1 (2023): 70-82.

6. Hoffmann, Michael R., et al. "Environmental applications of semiconductor photocatalysis." Chemical reviews 95.1 (1995): 69-96.

Table S1. Fluorescence region integrals (B, T: protein-like; A, M, C: humic-like) and EEM-derived indices (BIX, FI, HIX) for the raw textile wastewater and treated samples under UV or sunlight with/without CoAl–LDH/CoO_x and different H_2O_2 doses, corresponding to the conditions shown in Fig. 11.

Entry	Sample	B	T	A	M	C	BIX	FI	HIX
1	RWW	2.792517	5.53963	4.01545	2.020157	0.502247	1.854736	2.548598	0.163404
2	RWW-CoAl-LDH/CoOx photocatalyst-8.16 mM H_2O_2	0.826828	1.830609	0.52138	0.424152	0.145631	1.172786	1.507494	0.268705
3	RWW-CoAl-LDH/CoOx photocatalyst-16.32 mM H_2O_2-UV light	0.31732	0.930005	0.443913	0.418084	0.120315	1.040149	1.581192	0.416177
4	RWW- CoAl-LDH/CoOx photocatalyst-8.16 mM H_2O_2-Sunlight	4.678554	8.325116	1.275733	0.635039	0.174625	1.824623	1.871997	0.113486
5	RWW- CoAl-LDH/CoOx photocatalyst-16.32 mM H_2O_2-Sunlight	4.35808	7.783861	1.209332	0.60551	0.159034	1.850145	1.921704	0.116913
6	RWW- CoAl-LDH/CoOx photocatalyst-24.48 mM H_2O_2-Sunlight	4.6156	8.207937	1.255646	0.702668	0.205683	1.474142	2.130601	0.129949
7	RWW- no catalyst-8.16 mM H_2O_2- UV light	4.651966	8.799412	1.563659	0.836587	0.26993	1.572561	2.055127	0.126675
8	RWW- no catalyst -16.32 mM H_2O_2- UV light	4.38653	8.163297	1.493351	0.843729	0.353819	1.393227	2.152558	0.15301
9	RWW- no catalyst -24.48 mM H_2O_2- UV light	4.347157	8.280476	1.529621	0.860469	0.366017	1.429165	2.298544	0.140768